Engineering and Computational Mechanics
Volume 165 Issue EM2

Efficient single-step time-dependent analysis of PC structures
Si, Au and Tsang

ice | proceedings

Proceedings of the Institution of Civil Engineers
Engineering and Computational Mechanics 165 June 2012 Issue EM2
Pages 89–102 http://dx.doi.org/10.1680/eacm.10.00030
Paper 1000030
Received 10/08/2010 Accepted 07/12/2010
Keywords: cables & tendons/concrete structures/mathematical modelling

ice Institution of Civil Engineers publishing

Efficient single-step time-dependent analysis of PC structures

1 **Xue-tong Si** MPhil
PhD Student, Department of Civil Engineering, The University of Hong Kong, Hong Kong

2 **Francis T. K. Au** MSc(Eng), PhD, CEng, MICE, FIStructE, FHKIE
Professor, Department of Civil Engineering, The University of Hong Kong, Hong Kong

3 **Neil C. M. Tsang** PhD, CEng, MIStructE, MASCE
Senior Lecturer, Department of the Built Environment, Coventry University, Coventry, UK; Honorary Lecturer, Department of Civil and Environmental Engineering, Imperial College London, London, UK



This paper describes an efficient single-step method to predict the time-dependent behaviour of prestressed concrete (PC) structures due to concrete creep, concrete shrinkage and cable relaxation. A versatile tendon sub-element is first developed to model prestressing cables of arbitrary profiles. To enable accurate estimation of losses of cable forces, a new relaxation model is formulated based on the equivalent creep coefficient, which is verified to work not only in the case of intrinsic relaxation but also under various boundary conditions. An efficient single-step finite-element method is then devised for time-dependent analysis of PC structures considering creep, shrinkage and relaxation based on the age-adjusted elasticity modulus, shrinkage-adjusted elasticity modulus and relaxation-adjusted elasticity modulus respectively. The effects of creep, shrinkage and relaxation on the long-term performance of PC structures are investigated. The numerical results obtained indicate not only the accuracy of the method but also the significance of considering the interaction among various time-varying factors.

Notation

A	sectional area of element
E	elastic modulus of member
$\overline{E}$	adjusted elasticity modulus (AEM)
$\overline{E}_s(\Delta t)$	mean modulus of elasticity of tendon
$\{\boldsymbol{F}\}$	load vector of element under local coordinate system
f_{py}	'yield' stress of prestressing tendons
$\overline{G}$	adjusted shear modulus
$[\boldsymbol{H}]$	transfer matrix
L, l	lengths of element
$[\overline{\boldsymbol{K}}]$	stiffness matrix of a structure under global coordinate system
$[\boldsymbol{k}]$	local stiffness matrix
$[\overline{\boldsymbol{k}}]$	local stiffness matrix based on AEM
$[\boldsymbol{N}]$	matrix of shape functions
r	relaxation function
$[\boldsymbol{T}]$	transformation matrix
(t, t_0)	period from time t_0 to time t
(x, y, z)	nodal coordinates in local xyz system
$\{\Delta\boldsymbol{f}\}$	incremental load vector of element
$\{\Delta\boldsymbol{Q}\}$	incremental load vector of structure under global coordinate system
$\{\Delta\boldsymbol{q}^e\}$	incremental load vector of element under local coordinate system
$\{\Delta\boldsymbol{U}\}$	incremental displacement vector of structure under global coordinate system
$\{\Delta\boldsymbol{\delta}\}$	incremental displacement vector of element
$\Delta\varepsilon_{\phi s}(t)$	incremental creep strain
$\Delta\sigma_{pr}$	stress relaxation of tendon
$\{\boldsymbol{\delta}\}$	displacement vector of element
$\varepsilon(t)$	total strain of member at time t
σ_{p0}	initial stress level of prestressing tendon
$\sigma_s(t_0)$	stress applied at time t_0
φ	creep coefficient
χ	ageing coefficient

Subscripts

c	concrete
cc	concrete creep
cs	concrete shrinkage
c1	related to effects of concrete creep and/or cable relaxation only
c2	related to effects of concrete shrinkage and its interaction with creep only

s steel tendon
T tendon sub-element with respect to beam element
φc related to concrete creep
φs related to stress relaxation of tendons

1. Introduction

The creep and shrinkage of concrete and relaxation of cables in prestressed concrete (PC) structures are known to interact with one another. These time-dependent factors can cause the redistribution of internal forces, which in turn affects the long-term structural performance. It is thus important to predict the time-dependent deformations due to these effects reasonably accurately not only to ensure satisfactory structural performance but also to enable effective operation of structural health monitoring systems.

In time-dependent analysis using the finite-element method combined with time integration (Ghali *et al.*, 2002), the concrete members are usually modelled by frame elements and the tendons are treated as truss elements connected to the structural nodes with rigid arms (Aalami, 1998; Ariyawardena and Ghali, 2002; Au *et al.*, 2009; Elbadry and Ghali, 2001). If a curved cable is modelled as a series of straight truss elements, it requires the concrete member to be subdivided into the same number of frame elements, thus increasing the size of the problem. To improve the efficiency of time-dependent analysis, some single-step methods have been proposed, including the use of the age-adjusted elasticity modulus (AAEM) based on the relaxation function of concrete (Bažant, 1972), the shrinkage-adjusted elasticity modulus (SAEM) by introducing an ageing coefficient to account for the interaction between concrete creep and concrete shrinkage (Au *et al.*, 2007) and the history-adjusted elasticity modulus (HAEM) to account for stage construction (Au *et al.*, 2009). In time-dependent analysis of PC structures, the interactions among concrete creep, concrete shrinkage and cable relaxation are often considered approximately by introducing relaxation reduction coefficients taken from charts or tables (Ghali and Trevino, 1985; Sharif *et al.*, 1993; Tadros *et al.*, 1975), or by the equivalent time or reduction factor in Eurocode 2 (BSI, 2005). It is therefore desirable to develop better methods for modelling the interaction of cable relaxation with other effects.

This paper describes a more general single-step method to predict the time-dependent behaviour of PC structures considering creep, shrinkage and relaxation. Based on an efficient tendon sub-element to cope with cables with arbitrary profiles and an equivalent relaxation model for tendons, an efficient single-step method is developed for the time-dependent analysis of PC structures. Numerical examples are provided to validate the proposed method.

2. Modelling of frame members with cables of arbitrary profiles

The common assumptions for analysis of frame structures are made. The tendons are assumed to be perfectly bonded to the structural concrete members. The concrete, steel reinforcement and steel cable are modelled separately with connections at the nodes only, while ignoring their interaction within the element. It is also assumed that plane sections remain plane after bending. The present analysis is mainly for time-dependent behaviour of PC structures with full or limited prestressing, which are not expected to crack under working conditions. Figure 1 shows a straight spatial tendon sub-element a–b of length l_s over part of the length L_c of a spatial beam element 1–2 with three translational degrees of freedom (DOFs) and three rotational DOFs at each node. These DOFs are appended by the node number as appropriate. Note that the beam element and tendon sub-element need not be in the same plane. A right-handed local coordinate axis system *xyz* is chosen with the *x*-axis coincident with the member axis and the origin at node 1. The tendon sub-element a–b has three translational DOFs at each node with respect to the *x*-, *y*- and *z*-axes of the beam element. Nodes a and b of the tendon sub-element are connected to the beam element by rigid arms a–1′ and b–2′ perpendicular to the *x*-axis.

The displacement vector $\{\boldsymbol{\delta}_{ab}\}$ of tendon sub-element a–b is related to the displacement vector $\{\boldsymbol{\delta}_{1'2'}\}$ of segment 1′–2′ by

$$\{\boldsymbol{\delta}_{ab}\} = [\boldsymbol{H}]\{\boldsymbol{\delta}_{1'2'}\} \quad (1)$$

using the transfer matrix $[\boldsymbol{H}]$ obtained from the geometry (Ghali and Neville, 1989) in terms of the coordinates (x_1, y_1, z_1), (x_2, y_2, z_2), (x_a, y_a, z_a) and (x_b, y_b, z_b) of nodes 1, 2, a and b respectively in accordance with the local *x*-, *y*- and *z*-axes of the beam element. The displacement vector $\{\boldsymbol{\delta}_{1'2'}\}$ of segment 1′–2′ can be expressed in terms of the displacement vector $\{\boldsymbol{\delta}_{12}\}$ of beam element 1–2 and the matrix $[\boldsymbol{N}]$ (Logan, 2001) of shape functions and their derivatives evaluated at positions $x_{1'}$ and $x_{2'}$ as

$$\{\boldsymbol{\delta}_{1'2'}\} = [\boldsymbol{N}]\{\boldsymbol{\delta}_{12}\} \quad (2)$$

Relating the displacement vector $\{\boldsymbol{\delta}_{ab}\}$ of tendon sub-element

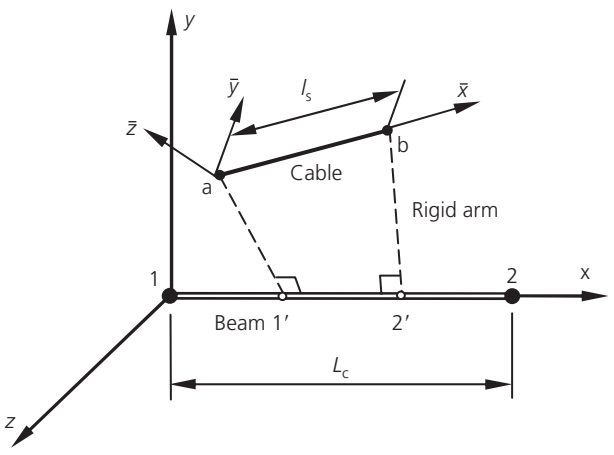

Figure 1. The proposed tendon element

a–b to the displacement vector $\{\boldsymbol{\delta}_{12}\}$ of beam element 1–2 by Equations 1 and 2, and using the conventional finite-element formulation, the stiffness matrix $[\boldsymbol{k}]_{\mathrm{T}}$ of the tendon sub-element with respect to the DOFs of the beam element can be expressed as

$$[\boldsymbol{k}]_{\mathrm{T}} = [\boldsymbol{N}]^{\mathrm{T}}[\boldsymbol{H}]^{\mathrm{T}}[\boldsymbol{T}]^{\mathrm{T}}[\boldsymbol{k}]_{\mathrm{s}}[\boldsymbol{T}][\boldsymbol{H}][\boldsymbol{N}] \quad 3.$$

in terms of the local stiffness matrix $[\boldsymbol{k}]_{\mathrm{s}}$ of the tendon and the transformation matrix $[\boldsymbol{T}]$, which comprises the direction cosines of element a–b in the *xyz*-system. The load vector $\{\boldsymbol{F}\}_{\mathrm{T}}$ of the tendon sub-element with respect to the DOFs of the beam element can similarly be expressed in terms of the local load vector $\{\boldsymbol{F}\}_{\mathrm{s}}$ as

$$\{\boldsymbol{F}\}_{\mathrm{T}} = [\boldsymbol{N}]^{\mathrm{T}}[\boldsymbol{H}]^{\mathrm{T}}[\boldsymbol{T}]^{\mathrm{T}}\{\boldsymbol{F}\}_{\mathrm{s}} \quad 4.$$

A cable of arbitrary profile can therefore be divided into a series of small tendon sub-elements without increasing the total number of DOFs of the entire structure. For example, the cable profile may be described by its eccentricities at regular intervals along the beam. Likewise, the forces in the tendon sub-elements can be specified to simulate approximately any variations of initial cable force along its length due to various sources of losses of prestress. Reinforcing bars can be modelled similarly by adopting straight profiles and taking the initial stress as zero.

3. Relaxation model for steel tendon

Relaxation is the phenomenon of gradual loss of stress in a stressed tendon. The loss of tension under constant strain, as in a test in which the length of tendon is kept constant after stretching, is referred to as intrinsic relaxation. Assuming a relatively constant temperature, it is desirable to express the stress relaxation $\Delta\sigma_{\mathrm{pr}}$ as a function of time t (hours) since stressing and initial stress level σ_{p0} for prestress loss analysis. An equation to evaluate the stress relaxation for stress-relieved strands (Magura *et al.*, 1964) is

$$\frac{\Delta\sigma_{\mathrm{pr}}}{\sigma_{\mathrm{p0}}} = -\frac{\log(t)}{10}\left(\frac{\sigma_{\mathrm{p0}}}{f_{\mathrm{py}}} - 0{\cdot}55\right) \quad 5.$$

where f_{py} is the 'yield' stress, taken as the stress at a strain of 0·01. For low-relaxation strands, the equation commonly used in North America (Youakim *et al.*, 2007) is

$$\frac{\Delta\sigma_{\mathrm{pr}}}{\sigma_{\mathrm{p0}}} = -\frac{\log(24t)}{40}\left(\frac{\sigma_{\mathrm{p0}}}{f_{\mathrm{py}}} - 0{\cdot}55\right) \quad 6.$$

Note that both Equations 5 and 6 assume that relaxation is negligible for initial stress ratios $\sigma_{\mathrm{p0}}/f_{\mathrm{py}}$ below 0·55.

Creep and shrinkage tend to reduce the length of a PC member, thereby reducing the tendon stress. To account for the effects of creep and shrinkage on relaxation approximately, most engineers have adopted reduced relaxation coefficients (Ghali *et al.*, 2002), relaxation factors from design codes such as BS 8110: Part 1 (BSI, 1997) or a constant reduction factor of 0·8 (BSI, 2005). It is therefore desirable to develop a more rational method for their interaction.

3.1 Equivalent creep coefficient of a steel tendon

When a tendon is stretched under a constant stress $\sigma_{\mathrm{s}}(t_0)$ applied at time t_0, the total strain $\varepsilon_{\mathrm{s}}(t)$ at time t, including the instantaneous and creep strains, is expressed in terms of the Young's modulus of elasticity E_{s} and equivalent creep coefficient $\varphi_{\mathrm{s}}(t,\ t_0)$ as

$$\varepsilon_{\mathrm{s}}(t) = \frac{\sigma_{\mathrm{s}}(t_0)}{E_{\mathrm{s}}}[1 + \varphi_{\mathrm{s}}(t,\ t_0)] \quad 7.$$

Au and Si (2011) have shown that the equivalent creep coefficient can simulate accurately the time-dependent behaviour of tendons under various boundary conditions, including the extreme cases of intrinsic relaxation when the strain is kept constant and free extension when the stress is kept constant. Although the creep coefficient $\varphi_{\mathrm{s}}(t,\ t_0)$ also depends on the initial prestressing ratio $\sigma_{\mathrm{s}}(t_0)/f_{\mathrm{py}}$, it is omitted from the notation for convenience. With the stress changing with time, the total strain of steel tendon $\varepsilon_{\mathrm{s}}(t)$ is obtained by summing the responses of $\mathrm{d}\sigma_{\mathrm{s}}(\tau)$ applied at time τ based on the principle of superposition, namely

$$\varepsilon_{\mathrm{s}}(t) = \frac{\sigma_{\mathrm{s}}(t_0)}{E_{\mathrm{s}}}[1 + \varphi_{\mathrm{s}}(t,\ t_0)] + \int_0^{\Delta\overline{\sigma}_{\mathrm{s}}(t)} \frac{1 + \varphi_{\mathrm{s}}(t,\ \tau)}{E_{\mathrm{s}}}\ \mathrm{d}\sigma_{\mathrm{s}}(\tau) \quad 8.$$

where $\Delta\overline{\sigma}_{\mathrm{s}}(t)$ is the stress increment from time t_0 to t. If the creep behaviour of the tendon is assumed to be independent of age, one can introduce the creep coefficient $\overline{\varphi}_{\mathrm{s}}(t - t_0) = \varphi_{\mathrm{s}}(t,\ t_0)$, so that Equation 8 can be rewritten as

$$\varepsilon_{\mathrm{s}}(t) = \frac{\sigma_{\mathrm{s}}(t_0)}{E_{\mathrm{s}}}[1 + \overline{\varphi}_{\mathrm{s}}(t - t_0)] + \int_0^{\Delta\overline{\sigma}_{\mathrm{s}}(t)} \frac{1 + \overline{\varphi}_{\mathrm{s}}(t - \tau)}{E_{\mathrm{s}}}\ \mathrm{d}\sigma_{\mathrm{s}}(\tau) \quad 9.$$

Using Equation 9 to write down $\varepsilon_{\mathrm{s}}(t + \Delta t)$ explicitly and obtaining the difference, the incremental strain $\Delta\varepsilon_{\mathrm{s}}(t)$ can be obtained in terms of the incremental stress $\Delta\sigma_{\mathrm{s}}(t)$, mean modulus of elasticity $\overline{E}_{\mathrm{s}}(\Delta t)$ and incremental creep strain $\Delta\varepsilon_{\varphi\mathrm{s}}(t)$ as

$$10.\quad \Delta\varepsilon_s(t) = \frac{\Delta\sigma_s(t)}{\overline{E}_s(\Delta t)} + \Delta\varepsilon_{\phi s}(t)$$

where

$$\Delta\varepsilon_s(t) = \varepsilon_s(t+\Delta t) - \varepsilon_s(t)$$

$$\Delta\sigma_s(t) = \sigma_s(t+\Delta t) - \sigma_s(t)$$

$$\overline{E}_s(\Delta t) = \frac{E_s}{1+\overline{\varphi}_s(\Delta t)/2}$$

$$\Delta\varepsilon_{\phi s} = \frac{\sigma_s(t_0)}{E_s}[\overline{\varphi}_s(t+\Delta t-t_0) - \overline{\varphi}_s(t-t_0)] + \int_{\sigma_s(t_0)}^{\sigma_s(t)} \frac{\overline{\varphi}_s(t+\Delta t-\tau) - \overline{\varphi}_s(t-\tau)}{E_s} \frac{d\sigma_s(\tau)}{d\tau} d\tau$$

For the case of intrinsic relaxation at constant strain, there is no change in strain with time (i.e. $\Delta\varepsilon_s(t) = 0$). Let Δt be the subsequent time interval after tensioning so as to define the instants $t_1 = t_0 + \Delta t, \ldots, t_n = t_0 + n\Delta t$. Applying Equation 10 to time $t = t_0$ and noting that $\Delta\varepsilon_s(t) = 0$, yields

$$11.\quad \overline{\varphi}_s(\Delta t) = \frac{-\Delta\sigma_s(t_0)}{\sigma_s(t_0) + \Delta\sigma_s(t_0)/2}$$

Repeating the same procedure, one can derive the creep coefficient at time t_n in terms of the previous values as

$$12.\quad \begin{aligned}\overline{\varphi}_s[(n+1)\Delta t] &= \frac{\sigma_s(t_0)\overline{\varphi}_s(n\Delta t)}{\sigma_s(t_0) + \Delta\sigma_s(t_0)/2} \\ &\quad - \frac{\Delta\sigma_s(t_0 + n\Delta t)\left[1 + \overline{\varphi}_s(\Delta t)/2\right]}{\sigma_s(t_0) + \Delta\sigma_s(t_0)/2} \\ &\quad - \frac{-\Delta\sigma_s(t_0)\overline{\varphi}_s[(n-1)\Delta t]/2}{\sigma_s(t_0) + \Delta\sigma_s(t_0)/2} \\ &\quad - \frac{\sum_{i=2}^{n}\{\Delta\sigma_s[t_0 + (i-1)\Delta t]/2\} \times \left\{\overline{\varphi}_s[(n-i+2)\Delta t] - \overline{\varphi}_s[(n-i)\Delta t]\right\}}{\sigma_s(t_0) + \Delta\sigma_s(t_0)/2}\end{aligned}$$

In other words, the equivalent creep coefficient can be calculated based on the intrinsic stress relaxation function.

3.2 Relaxation-adjusted elasticity modulus and ageing coefficient

Defining an ageing coefficient χ_s to account for the time-dependent effects due to tendon creep, which is also independent of age such that $\chi_s(t, t_0) = \overline{\chi}_s(t - t_0)$, Equation 9 can be rewritten as

$$13.\quad \varepsilon_s(t) = \frac{\sigma_s(t_0)}{E_s}[1 + \overline{\varphi}_s(t-t_0)] + \frac{\Delta\overline{\sigma}_s(t)}{E_s}[1 + \overline{\chi}_s(t-t_0)\,\overline{\varphi}_s(t-t_0)]$$

Let

$$\xi = \frac{\sigma_s(\tau) - \sigma_s(t_0)}{\Delta\overline{\sigma}_s(t)}$$

and then one has

$$\frac{d\sigma_s(\tau)}{d\tau} = \Delta\overline{\sigma}_s(t)\frac{d\xi}{d\tau}$$

By comparing Equation 9 with Equation 13, the ageing coefficient can be expressed in terms of the creep coefficient as

$$14.\quad \overline{\chi}_s(t-t_0) = \frac{1}{\overline{\varphi}_s(t-t_0)}\int_{t_0}^{t}\left[1 + \overline{\varphi}_s(t-\tau)\right]\frac{d\xi}{d\tau}d\tau - \frac{1}{\overline{\varphi}_s(t-t_0)}$$

The relaxation-adjusted elasticity modulus (RAEM) $\overline{E}_s(t-t_0)$ at time t can be expressed by reference to Equation 13 in terms of the ageing coefficient $\overline{\chi}_s(t-t_0)$ as

$$15.\quad \overline{E}_s(t-t_0) = \frac{E_s}{1 + \overline{\chi}_s(t-t_0)\overline{\varphi}_s(t-t_0)}$$

The standard constant-strain relaxation test is often the only available source of information on the time-dependent behaviour of tendons. Let $r_s(t, t_0)$ be the relaxation function, which is independent of age, so that one can write it in the form $\overline{r}_s(t-t_0) = r_s(t, t_0)$. If a tendon is stressed to $\sigma_s(t_0) = \varepsilon_s(t_0)E_s$ at time t_0 and the strain $\varepsilon_s(t_0)$ is kept constant, the variation of tendon stress $\sigma_s(t)$ can be expressed in terms of the relaxation function as

$$16.\quad \sigma_s(t) = \varepsilon_s(t_0)r_s(t, t_0) = \varepsilon_s(t_0)\overline{r}_s(t-t_0)$$

In a constant-strain relaxation test, the stress increment $\Delta\overline{\sigma}_s(t)$ appears as

$$17.\quad \Delta\overline{\sigma}_s(t) = \sigma_s(t) - \sigma_s(t_0)$$

Substituting Equations 16 and 17 into Equation 13, and noting that $\sigma_s(t_0) = \varepsilon_s(t_0)E_s$, the ageing coefficient can be obtained as

$$18. \quad \overline{\chi}_s(t - t_0) = \frac{1}{1 - \overline{r}_s(t - t_0)/E_s} - \frac{1}{\overline{\varphi}_s(t - t_0)}$$

4. Single-step method for time-dependent analysis

Although time integration provides a reliable method for time-dependent analysis, the computing time and memory requirement both increase drastically with the number of time steps because the time-dependent strains of concrete and tendons within a time interval depend on the loading history up to that time. To overcome this, it is desirable to develop single-step methods using adjusted elasticity moduli. It is assumed that the external loading remains unchanged during the time interval considered.

The stress–strain relationship of a tendon is obtained based on the RAEM by rewriting Equation 13 as

$$19. \quad \varepsilon_s(t) = \frac{\sigma_s(t_0)}{E_s}[1 + \overline{\varphi}_s(t - t_0)] + \frac{\Delta\overline{\sigma}_s(t)}{E_s(t - t_0)}$$

Introducing the incremental strain from time t_0 to t as

$$\Delta\varepsilon_s(t) = \varepsilon_s(t) - \sigma_s(t_0)/E_s$$

and rearranging, the corresponding incremental stress $\Delta\overline{\sigma}_s(t)$ can be obtained as

$$20. \quad \Delta\overline{\sigma}_s(t) = \overline{E}_s(t - t_0)\left[\Delta\varepsilon_s(t) - \frac{\sigma_s(t_0)}{E_s}\overline{\varphi}_s(t - t_0)\right]$$

The incremental load vector $\{\Delta\boldsymbol{q}^e\}$ from time t_0 to time t can be derived by the conventional finite-element method as

$$21. \quad \{\Delta\boldsymbol{q}^e\}_s = [\overline{\boldsymbol{k}}(t, t_0)]_s\{\Delta\boldsymbol{\delta}\}_s + \{\Delta\boldsymbol{f}(t, t_0)\}_{\phi s}$$

where $\{\Delta\boldsymbol{\delta}\}_s$ is the incremental displacement vector. The stiffness matrix $[\overline{\boldsymbol{k}}(t, t_0)]_s$ and the incremental load vector due to cable relaxation $\{\Delta\boldsymbol{f}(t, t_0)\}_{\phi s}$ are

$$22. \quad [\overline{\boldsymbol{k}}(t, t_0)]_s = \frac{\overline{E}_s(t - t_0)A_s}{l_s}\begin{bmatrix} 1 & -1 \\ -1 & 1 \end{bmatrix}$$

$$23. \quad \{\Delta\boldsymbol{f}(t, t_0)\}_{\phi s} = \frac{\overline{E}_s(t - t_0)}{E_s}\overline{\varphi}_s(t - t_0)\begin{Bmatrix} \bar{N}_s(t_0) \\ -\bar{N}_s(t_0) \end{Bmatrix}$$

where $\bar{N}_s(t_0)$ is the axial force of the element at time t_0.

Based on the principle of superposition, the total concrete strain $\varepsilon_c(t)$ due to the initial applied stress $\sigma_c(t_0)$, creep and shrinkage is given by

$$24. \quad \varepsilon_c(t) = \sigma_c(t_0)\left[\frac{1 + \varphi_c(t, t_0)}{E_c(t_0)}\right] + \int_0^{\Delta\overline{\sigma}_c(t)} \frac{1 + \varphi_c(t, \tau)}{E_c(\tau)}\, d\sigma_c(\tau) + \varepsilon_{cs}(t, t_0)$$

where $\phi_c(t, t_0)$ is the creep coefficient at time t for concrete loaded at time t_0, $E_c(t)$ is the modulus of elasticity of concrete at time t, $\Delta\overline{\sigma}_c(t)$ is the stress increment from time t_0 to t and $\varepsilon_{cs}(t, t_0)$ is the free shrinkage from time t_0 to t. To predict the long-term performance of concrete structures efficiently, one may solve the problem approximately in two separate parts as follows. The AAEM (Ghali *et al.*, 2002) is first used to account for the effects of initial stresses and creep, giving the strain component $\overline{\varepsilon}_{cc}(t)$ and 'creep' stress increment $\Delta\overline{\sigma}_{cc}(t)$. Then, the SAEM (Au *et al.*, 2009) is utilised to account for the interaction between shrinkage and creep, giving the strain component $\overline{\varepsilon}_{cs}(t)$ and 'shrinkage' stress increment $\Delta\overline{\sigma}_{cs}(t)$ with the zero initial strain condition $\overline{\varepsilon}_{cs}(t_0) = 0$. Therefore, noting the above conditions of strain

$$\varepsilon_c(t) = \overline{\varepsilon}_{cc}(t) + \overline{\varepsilon}_{cs}(t)$$

and stress increment

$$\Delta\overline{\sigma}_c(t) = \Delta\overline{\sigma}_{cc}(t) + \Delta\overline{\sigma}_{cs}(t)$$

Equation 24 gives the strain components $\overline{\varepsilon}_{cc}(t)$ and $\overline{\varepsilon}_{cs}(t)$ as

$$25. \quad \overline{\varepsilon}_{cc}(t) = \sigma_c(t_0)\left[\frac{1 + \varphi_c(t, t_0)}{E_c(t_0)}\right] + \frac{\Delta\overline{\sigma}_{cc}(t)}{\overline{E}_{cc}(t, t_0)}$$

$$26. \quad \overline{\varepsilon}_{cs}(t) = \frac{\Delta\overline{\sigma}_{cs}(t)}{\overline{E}_{cs}(t, t_0)} + \varepsilon_{cs}(t, t_0)$$

where the AAEM $\overline{E}_{cc}(t, t_0)$ is given in terms of the ageing coefficient χ_{cc} to account for creep by

$$\overline{E}_{cc}(t,\ t_0) = \frac{E_c(t_0)}{1 + \chi_{cc}\varphi_c(t,\ t_0)} \tag{27}$$

and the SAEM $\overline{E}_{cs}(t,\ t_0)$ is given in terms of the shrinkage coefficient χ_{cs} by

$$\overline{E}_{cs}(t,\ t_0) = \frac{E_c(t_0)}{1 + \chi_{cs}\varphi_c(t,\ t_0)} \tag{28}$$

The ageing coefficient χ_{cc} to account for concrete creep can be expressed in terms of the relaxation function $r_{cc}(t,\ t_0)$, initial Young's modulus $E_c(t_0)$ at time t_0 and creep coefficient $\varphi_c(t,\ t_0)$ (Ghali *et al.*, 2002) as

$$\chi_{cc}(t,\ t_0) = \frac{1}{1 - [r_{cc}(t,\ t_0)/E_c(t_0)]} - \frac{1}{\varphi_c(t,\ t_0)} \tag{29}$$

Similarly, the shrinkage coefficient χ_{cs} can be written in terms of the stressing function $s(t,\ t_0)$, shrinkage strain $\varepsilon_{cs}(t,\ t_0)$, initial Young's modulus $E_c(t_0)$ at time t_0 and concrete creep coefficient $\varphi_c(t,\ t_0)$ (Au *et al.*, 2009) as

$$\chi_{cs}(t,\ t_0) = -\frac{E_c(t_0)\varepsilon_{cs}(t,\ t_0)}{s(t,\ t_0)\varphi_c(t,\ t_0)} - \frac{1}{\varphi_c(t,\ t_0)} \tag{30}$$

The ageing coefficient χ_{cc} and shrinkage coefficient χ_{cs} for any arbitrary period $(t,\ t_0)$ can be calculated by time integration. First, by noting that the initial strain

$$\varepsilon_c(t_0) = \sigma_c(t_0)/E_c(t_0)$$

and incremental strain

$$\Delta\overline{\varepsilon}_{cc}(t) = \overline{\varepsilon}_{cc}(t) - \varepsilon_c(t_0)$$

further rearrangement of Equation 27 gives the creep stress increment $\Delta\overline{\sigma}_{cc}(t)$ as

$$\Delta\overline{\sigma}_{cc}(t) = \overline{E}_{cc}(t,\ t_0)[\Delta\overline{\varepsilon}_{cc}(t) - \varepsilon_c(t_0)\varphi_c(t,\ t_0)] \tag{31}$$

The incremental load vector $\{\Delta\boldsymbol{q}^e\}_{cc}$ of a beam element from time t_0 to t due to creep can be written in terms of the stiffness matrix $[\overline{\boldsymbol{k}}(t,\ t_0)]_{cc}$, the incremental creep displacement vector $\{\Delta\boldsymbol{\delta}\}_{cc}$ and the incremental load vector due to creep $\{\Delta\boldsymbol{f}(t,\ t_0)\}_{\phi c}$ as

$$\{\Delta\boldsymbol{q}^e\}_{cc} = [\overline{\boldsymbol{k}}(t,\ t_0)]_{cc}\{\Delta\boldsymbol{\delta}\}_{cc} + \{\Delta\boldsymbol{f}(t,\ t_0)\}_{\phi c} \tag{32}$$

The stiffness matrix $[\overline{\boldsymbol{k}}(t,\ t_0)]_{cc}$ is given by

$$[\overline{\boldsymbol{k}}]_{cc} = \begin{bmatrix} [\overline{\boldsymbol{k}}_{11}]_{cc} & [\overline{\boldsymbol{k}}_{12}]_{cc} \\ [\overline{\boldsymbol{k}}_{21}]_{cc} & [\overline{\boldsymbol{k}}_{22}]_{cc} \end{bmatrix} \tag{33a}$$

$$[\overline{\boldsymbol{k}}_{11}]_{cc} = \begin{bmatrix} \frac{A_c\overline{E}_{cc}}{L_c} & 0 & 0 & 0 & 0 & 0 \\ 0 & \frac{12\overline{E}_{cc}I_{cz}}{L_c^3} & 0 & 0 & 0 & \frac{6\overline{E}_{cc}I_{cz}}{L_c^2} \\ 0 & 0 & \frac{12\overline{E}_{cc}I_{cy}}{L_c^3} & 0 & -\frac{6\overline{E}_{cc}I_{cy}}{L_c^2} & 0 \\ 0 & 0 & 0 & \frac{\overline{G}_{cc}J_c}{L_c} & 0 & 0 \\ 0 & 0 & -\frac{6\overline{E}_{cc}I_{cy}}{L_c^2} & 0 & \frac{4\overline{E}_{cc}I_{cy}}{L_c} & 0 \\ 0 & \frac{6\overline{E}_{cc}I_{cz}}{L_c^2} & 0 & 0 & 0 & \frac{4\overline{E}_{cc}I_{cz}}{L_c} \end{bmatrix} \tag{33b}$$

$$[\overline{\boldsymbol{k}}_{21}]_{\mathrm{cc}} = [\overline{\boldsymbol{k}}_{12}]_{\mathrm{cc}}^{\mathrm{T}} = \begin{bmatrix} -\frac{A_{\mathrm{c}}\overline{E}_{\mathrm{cc}}}{L_{\mathrm{c}}} & 0 & 0 & 0 & 0 & 0 \\ 0 & -\frac{12\overline{E}_{\mathrm{cc}}I_{\mathrm{c}z}}{L_{\mathrm{c}}^3} & 0 & 0 & 0 & -\frac{6\overline{E}_{\mathrm{cc}}I_{\mathrm{c}z}}{L_c^2} \\ 0 & 0 & -\frac{12\overline{E}_{\mathrm{cc}}I_{\mathrm{c}y}}{L_{\mathrm{c}}^3} & 0 & \frac{6\overline{E}_{\mathrm{cc}}I_{\mathrm{c}y}}{L_{\mathrm{c}}^2} & 0 \\ 0 & 0 & 0 & -\frac{\overline{G}_{\mathrm{cc}}J_{\mathrm{c}}}{L_{\mathrm{c}}} & 0 & 0 \\ 0 & 0 & -\frac{6\overline{E}_{\mathrm{cc}}I_{\mathrm{c}y}}{L_{\mathrm{c}}^2} & 0 & \frac{2\overline{E}_{\mathrm{cc}}I_{\mathrm{c}y}}{L_{\mathrm{c}}} & 0 \\ 0 & \frac{6\overline{E}_{\mathrm{cc}}I_{\mathrm{c}z}}{L_{\mathrm{c}}^2} & 0 & 0 & 0 & \frac{2\overline{E}_{\mathrm{cc}}I_{\mathrm{c}z}}{L_{\mathrm{c}}} \end{bmatrix} \tag{33c}$$

$$[\overline{\boldsymbol{k}}_{22}]_{\mathrm{cc}} = \begin{bmatrix} \frac{A_{\mathrm{c}}\overline{E}_{\mathrm{cc}}}{L_{\mathrm{c}}} & 0 & 0 & 0 & 0 & 0 \\ 0 & \frac{12\overline{E}_{\mathrm{cc}}I_{\mathrm{c}z}}{L_{\mathrm{c}}^3} & 0 & 0 & 0 & -\frac{6\overline{E}_{\mathrm{cc}}I_{\mathrm{c}z}}{L_{\mathrm{c}}^2} \\ 0 & 0 & \frac{12\overline{E}_{\mathrm{cc}}I_{\mathrm{c}y}}{L_{\mathrm{c}}^3} & 0 & \frac{6\overline{E}_{\mathrm{cc}}I_{\mathrm{c}y}}{L_c^2} & 0 \\ 0 & 0 & 0 & \frac{\overline{G}_{\mathrm{cc}}J_{\mathrm{c}}}{L_{\mathrm{c}}} & 0 & 0 \\ 0 & 0 & \frac{6\overline{E}_{\mathrm{cc}}I_{\mathrm{c}y}}{L_{\mathrm{c}}^2} & 0 & \frac{4\overline{E}_{\mathrm{cc}}I_{\mathrm{c}y}}{L_{\mathrm{c}}} & 0 \\ 0 & -\frac{6\overline{E}_{\mathrm{cc}}I_{\mathrm{c}z}}{L_{\mathrm{c}}^2} & 0 & 0 & 0 & \frac{4\overline{E}_{\mathrm{cc}}I_{\mathrm{c}z}}{L_{\mathrm{c}}} \end{bmatrix} \tag{33d}$$

where $\overline{E}_{\mathrm{cc}}$ is the AAEM given by Equation 27, $\overline{G}_{\mathrm{cc}}$ is the age-adjusted shear modulus given in terms of Poisson's ratio ν_{c}

$$\overline{G}_{\mathrm{c}}(t) = \frac{\overline{E}_{\mathrm{cc}}(t)}{2(1+\nu_{\mathrm{c}})} \tag{34}$$

L_{c} is the length of element, A_{c} is the cross-sectional area, $I_{\mathrm{c}y}$ and $I_{\mathrm{c}z}$ are the second moments of area about the y- and z-axes respectively and J_{c} is the torsional constant. The incremental load vector due to creep $\{\Delta\boldsymbol{f}(t, t_0)\}_{\phi\mathrm{c}}$ is given by

$$\{\Delta\boldsymbol{f}\}_{\phi\mathrm{c}} = \begin{Bmatrix} \{\Delta\boldsymbol{f}_1\}_{\phi\mathrm{c}} \\ \{\Delta\boldsymbol{f}_2\}_{\phi\mathrm{c}} \end{Bmatrix} \tag{35a}$$

$$\{\Delta \boldsymbol{f}_1\}_{\phi c} = -\frac{\overline{E}_{cc}(t,\ t_0)}{E_c(t_0)}\varphi_c(t,\ t_0)\left(\begin{Bmatrix} \bar{N}_c(t_0) \\ [-\bar{M}_{c1}(t_0)+\bar{M}_{c2}(t_0)]/L_c \\ [-\bar{M}_{c3}(t_0)+\bar{M}_{c4}(t_0)]/L_c \\ \bar{T}_c(t_0) \\ -\bar{M}_{c3}(t_0) \\ -\bar{M}_{c1}(t_0) \end{Bmatrix} + \int_0^1 \begin{Bmatrix} N_{c0}(\bar{x}) \\ 6(2\bar{x}-1)M_{c0}(\bar{x})/L_c \\ 6(2\bar{x}-1)M_{c0}(\bar{x})/L_c \\ T_{c0}(\bar{x}) \\ 2(3\bar{x}-2)M_{c0}(\bar{x})/L_c \\ 2(3\bar{x}-2)M_{c0}(\bar{x})/L_c \end{Bmatrix} d\bar{x}\right) \tag{35b}$$

$$\{\Delta \boldsymbol{f}_2\}_{\phi c} = -\frac{\overline{E}_{cc}(t,\ t_0)}{E_c(t_0)}\varphi_c(t,\ t_0)\left(\begin{Bmatrix} -\bar{N}_c(t_0) \\ [\bar{M}_{c1}(t_0)-\bar{M}_{c2}(t_0)]/L_c \\ [\bar{M}_{c3}(t_0)-\bar{M}_{c4}(t_0)]/L_c \\ -\bar{T}_c(t_0) \\ \bar{M}_{c4}(t_0) \\ \bar{M}_{c2}(t_0) \end{Bmatrix} + \int_0^1 \begin{Bmatrix} -N_{c0}(\bar{x}) \\ 6(1-2\bar{x})M_{c0}(\bar{x})/L_c \\ 6(1-2\bar{x})M_{c0}(\bar{x})/L_c \\ -T_{c0}(\bar{x}) \\ 2(3\bar{x}-1)M_{c0}(\bar{x})/L_c \\ 2(3\bar{x}-1)M_{c0}(\bar{x})/L_c \end{Bmatrix} d\bar{x}\right) \tag{35c}$$

where the location of a point in the element is defined by $\bar{x} = x/L_c$, $_c(t_0)$ is the axial force at time t_0, $_c(t_0)$ is the torsional moment at time t_0, $_{c1}(t_0)$ and $_{c2}(t_0)$ are the bending moments about the z-axis of element at time t_0 ($t_0 \leqslant t$) at the ends $\bar{x} = 0$ and $\bar{x} = 1$ respectively, and $_{c3}(t_0)$ and $_{c4}(t_0)$ are the corresponding end moments about the y-axis. The time-independent forces $N_{c0}(\bar{x})$ and $T_{c0}(\bar{x})$ can be calculated from applied loads assuming both ends of the element to be fixed, while the time-independent moment, $M_{c0}(\bar{x})$ can be calculated from applied loads assuming the element to be simply supported. If all loads act at the nodes only, the integral in Equation 35 involving the time-independent terms will disappear.

Second, noting that the incremental strain

$$\Delta\bar{\varepsilon}_{cs}(t) = \bar{\varepsilon}_{cs}(t) - \bar{\varepsilon}_{cs}(t_0)$$

and the zero initial strain condition $\bar{\varepsilon}_{cs}(t_0) = 0$, the shrinkage stress increment $\Delta\bar{\sigma}_{cs}(t)$ can be obtained by rearranging Equation 28 as

$$\Delta\bar{\sigma}_{cs}(t) = \overline{E}_{cs}(t,\ t_0)[\Delta\bar{\varepsilon}_{cs}(t) - \varepsilon_{cs}(t,\ t_0)] \tag{36}$$

The incremental load vector $\{\Delta \boldsymbol{q}^e\}_{cs}$ of a beam element from time t_0 to t due to shrinkage can be written as

$$\{\Delta \boldsymbol{q}^e\}_{cs} = [\bar{\boldsymbol{k}}(t,\ t_0)]_{cs}\{\Delta\boldsymbol{\delta}\}_{cs} + \{\Delta \boldsymbol{f}(t,\ t_0)\}_{cs} \tag{37}$$

where $\{\Delta\boldsymbol{\delta}\}_{cs}$ is the incremental shrinkage displacement vector, the stiffness matrix $[\bar{\boldsymbol{k}}(t,\ t_0)]_{cs}$ is given by the right-hand side of Equation 33a except that $\overline{E}_{cs}(t,\ t_0)$ replaces $\overline{E}_{cc}$ and $\overline{G}_{cs}(t,\ t_0) = \overline{E}_{cs}(t,\ t_0)/2(1+\nu_c)$ replaces $\overline{G}_{cc}$, and the incremental load vector due to shrinkage $\{\Delta \boldsymbol{f}(t,\ t_0)\}_{cs}$ is given by

$$\{\Delta \boldsymbol{f}(t,\ t_0)\}_{cs} = -\overline{E}_{cs}(t,\ t_0)\varepsilon_{cs}(t,\ t_0) \times [1\ \ 0\ \ 0\ \ 0\ \ 0\ \ 0\ \ -1\ \ 0\ \ 0\ \ 0\ \ 0\ \ 0]^T \tag{38}$$

For beams provided with tendons, the AAEM, SAEM and RAEM can be used together to provide a convenient single-step solution consisting of two parts. For part 1 of the solution, which deals with concrete creep and cable relaxation only, the incremental load vector $\{\Delta \boldsymbol{q}^e\}_{c1}$ can be written as

$$\begin{aligned}\{\Delta \boldsymbol{q}^e\}_{c1} = &\left([\bar{\boldsymbol{k}}(t,\ t_0)]_{cc} + \sum_n [\bar{\boldsymbol{k}}(t,\ t_0)]_T\right)\{\Delta\boldsymbol{\delta}\}_{c1} \\ &+ \{\Delta \boldsymbol{f}(t,\ t_0)\}_{\phi c} \\ &+ [\boldsymbol{N}]^T[\boldsymbol{H}]^T[\boldsymbol{T}]^T\{\Delta \boldsymbol{f}(t,\ t_0)\}_{\phi s}\end{aligned} \tag{39}$$

where $\{\Delta\boldsymbol{\delta}\}_{c1}$ is the corresponding incremental nodal displacement vector and $[\bar{\boldsymbol{k}}(t,\ t_0)]_T$ is the stiffness matrix of the tendon sub-element with respect to the DOFs of the associated beam element, which can be calculated in a similar form as Equation 3 from the tendon stiffness matrix $[\bar{\boldsymbol{k}}(t,\ t_0)]_s$ based on the RAEM $\overline{E}_s(t - t_0)$ as

$$[\bar{\boldsymbol{k}}(t,\ t_0)]_T = [\boldsymbol{N}]^T[\boldsymbol{H}]^T[\boldsymbol{T}]^T[\bar{\boldsymbol{k}}(t,\ t_0)]_s[\boldsymbol{T}][\boldsymbol{H}][\boldsymbol{N}] \tag{40}$$

For part 2 of the solution which deals with concrete shrinkage and its interaction with concrete creep only, the incremental load vector $\{\Delta \boldsymbol{q}^e\}_{c2}$ can be written as

$$\{\Delta \boldsymbol{q}^e\}_{c2} = \left([\bar{\boldsymbol{k}}(t,\ t_0)]_{cs} + \sum_n [\boldsymbol{k}]_T\right)\{\Delta\boldsymbol{\delta}\}_{c2} + \{\Delta \boldsymbol{f}(t,\ t_0)\}_{cs} \tag{41}$$

where $\{\Delta\boldsymbol{\delta}\}_{c2}$ is the corresponding incremental nodal displacement vector and $[\boldsymbol{k}]_T$ is the elastic stiffness matrix of the tendon sub-element with respect to the DOFs of the associated beam element, which can be calculated by Equation 3.

The procedures to carry out single-step prediction of time-dependent behaviour of PC structures are summarised as follows.

(*a*) Elastic analysis is first carried out for time t_0. This involves the formulation of element stiffness matrices and load vectors, their transformation to suit the global coordinate system, assembly of the global stiffness matrix and load vector, and solution of the matrix equation.
(*b*) For the period from time t_0 to t, calculate the local stiffness matrix $[\overline{\boldsymbol{k}}(t, t_0)]_{cc}$ and the incremental load vector $\{\Delta\boldsymbol{f}(t, t_0)\}_{\phi c}$ of each beam element using the AAEM $\overline{E}_{cc}(t, t_0)$. Similarly calculate the stiffness matrix $[\overline{\boldsymbol{k}}(t, t_0)]_T$ and the incremental load vector $\{\Delta\boldsymbol{f}(t, t_0)\}_{\phi s}$ of each tendon sub-element with respect to the DOFs of the associated beam element using the RAEM $\overline{E}_s(t - t_0)$. After combining them for each of the beam elements, they are transformed to the global coordinate system and assembled to form the global stiffness matrix $[\overline{\boldsymbol{K}}(t, t_0)]_{c1}$ and the global incremental load vector $\{\Delta\boldsymbol{Q}\}_{c1}$, which account for concrete creep and cable relaxation. The incremental displacement vector $\{\Delta\boldsymbol{U}\}_{c1}$ due to concrete creep and cable relaxation from time t_0 to t can be solved from $[\overline{\boldsymbol{K}}(t, t_0)]_{c1}\{\Delta\boldsymbol{U}\}_{c1} = \{\Delta\boldsymbol{Q}\}_{c1}$. The incremental internal forces can be determined from the displacements accordingly.
(*c*) Again for the period from time t_0 to t, calculate the local stiffness matrix $[\overline{\boldsymbol{k}}(t, t_0)]_{cs}$ and the incremental load vector $\{\Delta\boldsymbol{f}(t, t_0)\}_{cs}$ of each beam element using the SAEM $\overline{E}_{cs}(t, t_0)$. Calculate the elastic stiffness matrix $[\overline{\boldsymbol{k}}]_T$ of each tendon sub-element with respect to the DOFs of the associated beam element. After combining them for each of the beam elements, they are transformed to the global coordinate system and assembled to form the global stiffness matrix $[\overline{\boldsymbol{K}}(t, t_0)]_{c2}$ and the global incremental load vector $\{\Delta\boldsymbol{Q}\}_{c2}$, which account for the effect of concrete shrinkage and its interaction with concrete creep. The incremental displacement vector $\{\Delta\boldsymbol{U}\}_{c2}$ under such effect from time t_0 to t can be solved from $[\overline{\boldsymbol{K}}(t, t_0)]_{c2}\{\Delta\boldsymbol{U}\}_{c2} = \{\Delta\boldsymbol{Q}\}_{c2}$. The incremental internal forces can be determined from the displacements accordingly.
(*d*) The incremental displacements and incremental internal forces from time t_0 to t can be obtained by adding together the corresponding quantities obtained from items (*b*) and (*c*) above.

5. Case studies

5.1 Equivalent creep coefficients of steel tendons

Let the initial prestressing ratio of a tendon be defined as $R = \sigma_s(t_0)/f_{py}$ in terms of initial prestress $\sigma_s(t_0)$ and 'yield' stress of the tendon f_{py}. Consider a prestressing tendon of unit length fixed at two ends. Based on the stress relaxation functions in Equations 5 and 6, the creep coefficients, ageing coefficients, stress relaxation and RAEM of stress-relieved and low-relaxation tendons under various initial prestressing ratios R of 0·7–0·9 were evaluated over 10 years. The time interval adopted was 8·76 h (one thousandth of a year) while the 'yield' strength was 1670 MPa. Various computed parameters of a typical perfectly fixed low-relaxation tendon are shown in Figure 2. Figure 2(a) shows the equivalent creep coefficients evaluated for various values of R. The perfect agreement between the simulated stress relaxation (symbols) and the theoretical intrinsic relaxation (curves) is shown in Figure 2(b). Figure 2(c) shows that the ageing coefficients for the three values of R are virtually the same. The values of RAEM normalised by the Young's modulus E_s are shown in Figure 2(d).

The same parameters were computed for two typical perfectly fixed stress-relieved and low-relaxation tendons with $R = 0{\cdot}8$ (Figure 3). The results show that the creep coefficients and cable relaxations increase with time, while the RAEMs decrease with time. A higher initial prestressing ratio increases the creep coefficient and cable relaxation but reduces the RAEM. The ageing coefficients of prestressing tendons are independent of the initial prestressing ratios and types of tendon. Figure 3 shows that low-relaxation tendons have lower creep coefficients and lower intrinsic stress relaxation but higher RAEMs than those of stress-relieved tendons, which demonstrates the superiority of the low-relaxation tendons.

5.2 Time-dependent analysis of PC beams

Figure 4 shows the PC beams with limited prestressing investigated for

(*a*) case 1, a simply supported beam with a straight tendon
(*b*) case 2, a simply supported beam with a parabolic tendon
(*c*) case 3, a two-span continuous beam with a deflected tendon.

In these verification examples, the non-prestressed steel is ignored. The necessary input parameters were as follows. All the beams had the same cross-section, with $b = 0{\cdot}6$ m and depth $h = 1{\cdot}2$ m. The characteristic compressive strength of the concrete f_{ck} was 32 MPa. Curing was provided until the age of $T_s = 3$ days, when shrinkage began. The relative humidity (RH) was taken as 80%. Each beam was provided with a stress-relieved tendon with a cross-sectional area A_s of 924×10^{-6} m^2 and Young's modulus E_s of 195 GPa. Each beam was post-tensioned at the age of $T_{c0} = 28$ days to an initial prestressing force P_t of 1108 kN with an initial prestressing ratio $R = 0{\cdot}8$ and grouted immediately afterwards. For simplicity, losses due to friction and anchorage draw-in are ignored. To enable accurate modelling of relaxation, the period from day 28 to day 365 was divided into 10 000 time steps for evaluation of the equivalent creep coefficient of the tendon. The parameters of CEB-FIP model code 1990 (CEB, 1993) were adopted in the calculation. The unit weight of beam was taken as 24·5 kN/m^3.

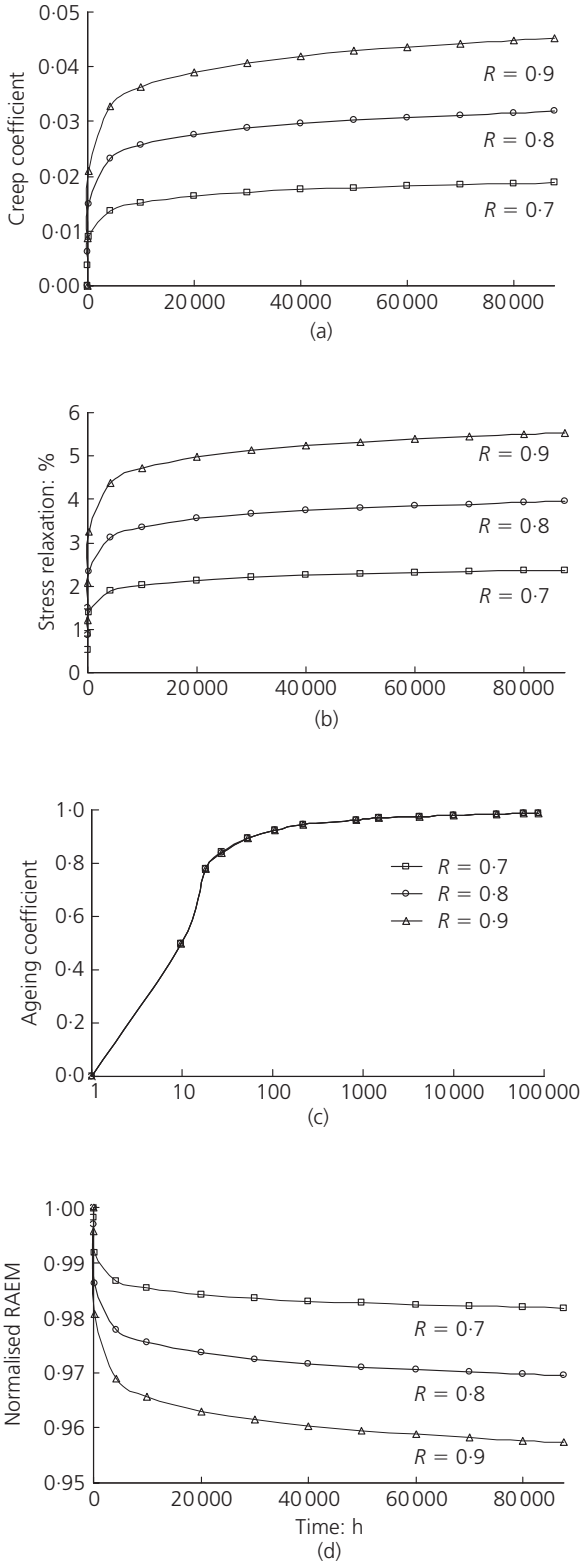

Figure 2. Computed parameters of a perfectly fixed low-relaxation tendon: (a) equivalent creep coefficients; (b) comparison of simulated stress relaxation (symbols) with theoretical values (curves); (c) ageing coefficients; (d) normalised RAEMs

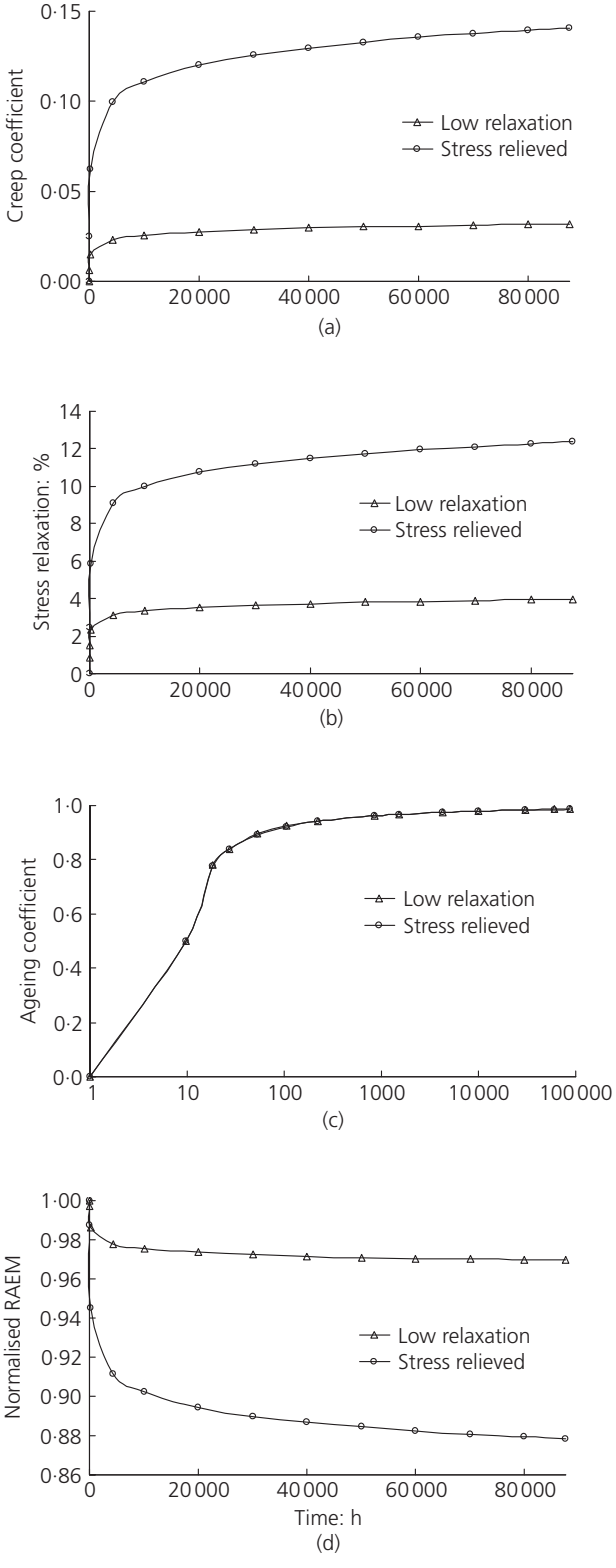

Figure 3. Comparison of computed properties of typical perfectly fixed stress-relieved and low-relaxation tendons with $R = 0{\cdot}8$: (a) equivalent creep coefficients; (b) comparison of simulated stress relaxation (symbols) with theoretical values (curves); (c) ageing coefficients; (d) normalised RAEMs

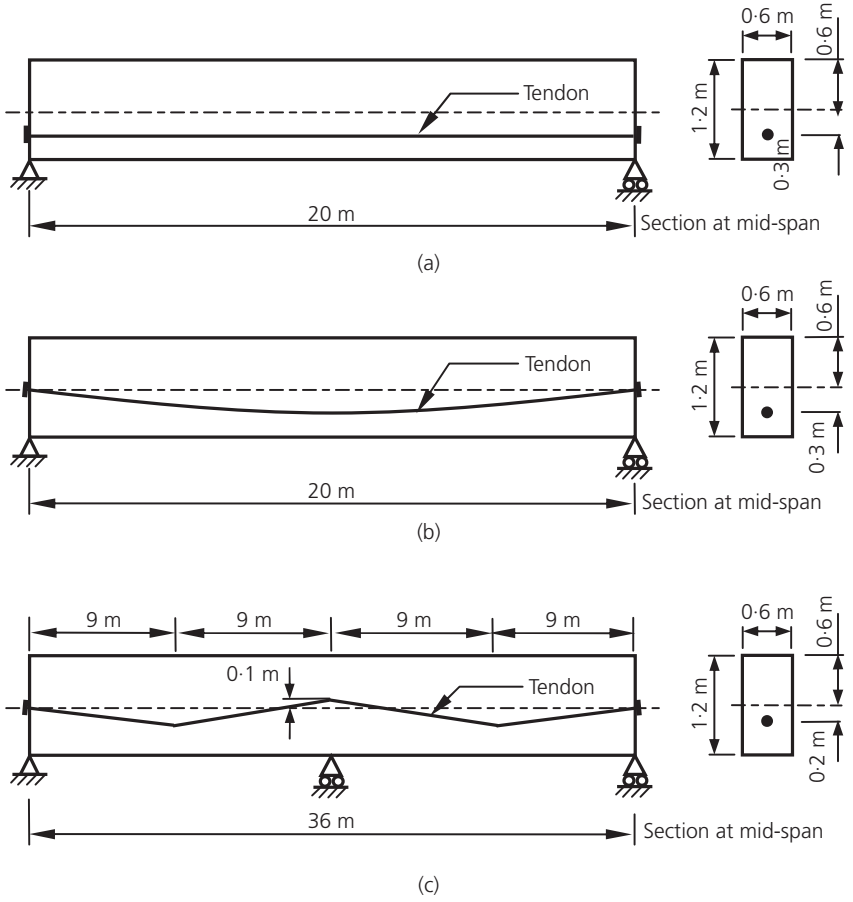

Figure 4. Post-tensioned beams investigated (not to scale).
(a) Case 1: a simply supported beam with a straight tendon.
(b) Case 2: a simply supported beam with a parabolic tendon.
(c) Case 3: a two-span continuous beam with a deflected tendon

The total deformations at day 365 of all three PC beams were then calculated by both the time integration and single-step methods using the discretisation schemes shown in Table 1. Apart from the time integration method, the single-step method also needs simple time marching to evaluate various effective moduli. The period from day 28 to day 365 was divided into 10–8000 equal time steps to investigate its effects on the accuracy of results. Fairly rapid convergence was observed in all cases, with reasonable results given by as few as ten time steps. The typical results of axial shortening along the centroidal axis and mid-span deflection of the simply supported beam with a straight tendon (i.e. case 1) are shown in Figure 5. Taking the results of time integration as benchmark solutions, the percentage errors of the single-step method obtained from 8000 equal time steps were calculated and are shown in Table 1. The maximum discrepancies in axial shortening and mid-span camber are 1·10% and −1·25% respectively, which demonstrates reasonably good agreement.

The time-dependent behaviour of the simply supported beam with a parabolic tendon (i.e. case 2) within the first year was then studied by both the time integration and single-step methods. In the time integration method, the period from $t_0 = 28$ days to $t = 365$ days was divided into 2000 equal time steps. In the single-step method, the same step size was used for computation of the effective moduli and prediction of the behaviour at time t is always started from $t_0 = 28$ days. The variations of axial shortening along the centroidal axis and mid-span deflection upon prestressing due to concrete creep, concrete shrinkage and cable relaxation are shown in Figure 6, giving discrepancies of 1·01% and −0·87% respectively. In general, the single-step method can be considered an efficient and accurate prediction method.

To investigate the effects of various factors on the time-dependent deformation, estimates of the axial shortening and mid-span deflection of the simply supported beam with a parabolic tendon (i.e. case 2) were determined for various hypothetical scenarios. Figure 7 shows the hypothetical estimates of axial shortening and mid-span deflection due to concrete creep, concrete shrinkage with and without cable relaxation calculated using the single-step method. The hypothetical estimates of loss of prestress due to

Case	Number of elements/sub-elements		Error: %	
	Equal-length beam elements	Tendon sub-elements	Axial shortening	Vertical camber at mid-span
1	10	40	1·07	−1·25
2	10	40	1·10	−0·93
3	4	4	0·88	−0·85

Table 1. Comparison of results from single-step method against time integration method

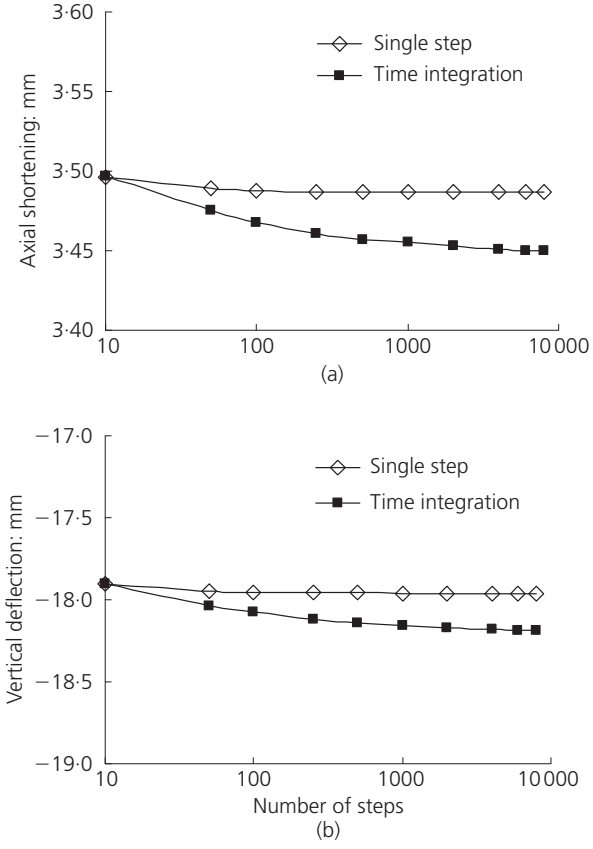

Figure 5. PC beam with straight tendon (case 1): effects of step size on deformations. (a) Axial shortening along centroidal axis at day 365; (b) mid-span deflection at day 365

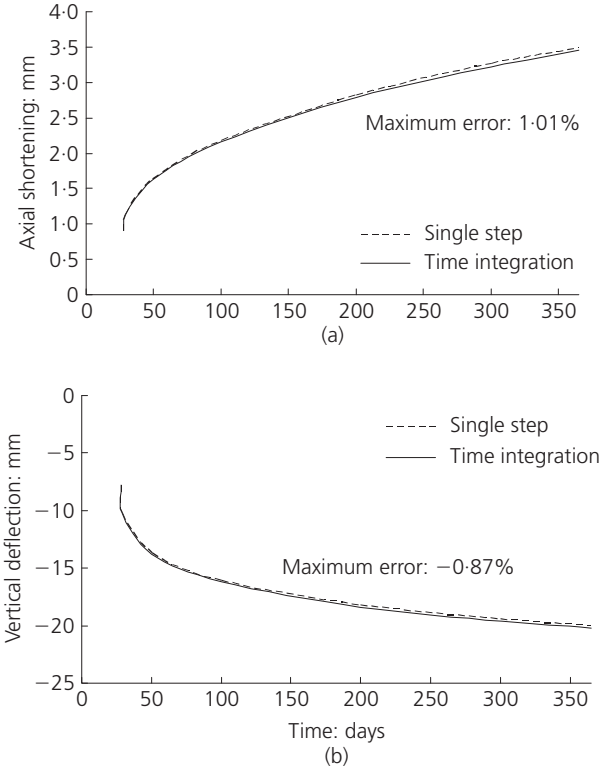

Figure 6. PC beam with parabolic tendon (case 2): comparison of deformations. (a) Axial shortening along centroidal axis; (b) mid-span deflection

cable relaxation with and without concrete creep and shrinkage calculated using the single-step method are shown in Figure 8. It is observed that cable relaxation reduces the axial shortening but increases the mid-span deflection due to concrete creep and concrete shrinkage after 1 year by 6·97% and 9·01% respectively. Concrete creep and shrinkage also increase the loss of prestress due to cable relaxation by 8·97%. Therefore, interactions among concrete creep, concrete shrinkage and cable relaxation should be considered carefully in time-dependent analyses of concrete structures.

6. Conclusions

This paper has described a general single-step method to predict the time-dependent behaviour of concrete structures due to concrete creep, concrete shrinkage and cable relaxation. The single-step method makes use of the relaxation-adjusted elasticity modulus for tendons, introduced in this paper, and the well-

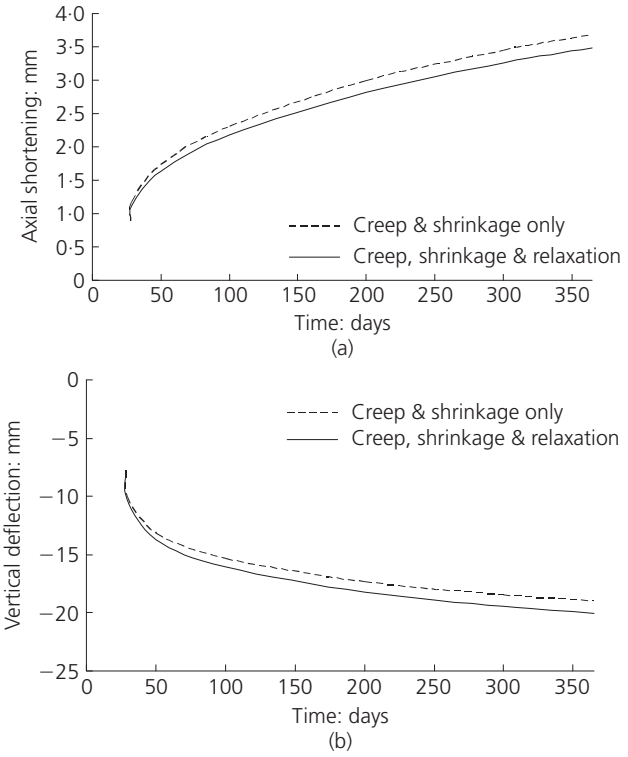

Figure 7. PC beam with parabolic tendon (case 2): effects of various factors on deformations. (a) Axial shortening along centroidal axis; (b) mid-span deflection

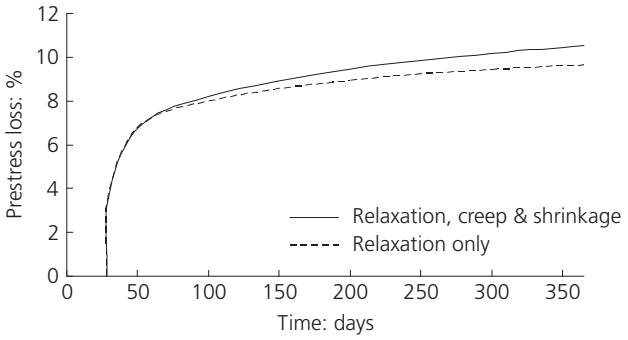

Figure 8. PC beam with parabolic tendon (case 2): effects of various factors on loss of prestress

established age-adjusted elasticity modulus and shrinkage-adjusted elasticity modulus for concrete members. Case studies indicate that the single-step method is an efficient and reliable method for time-dependent analysis of concrete structures. The results also show that concrete creep and shrinkage generally increase the loss of prestress while cable relaxation tends to reduce the time-dependent deformation due to concrete creep and shrinkage. Therefore, in order to carry out accurate time-dependent analyses of concrete structures, interactions among concrete creep, concrete shrinkage and cable relaxation should be carefully considered.

Acknowledgement

The work described in this paper was supported by the Research Grants Council (RGC) of the Hong Kong Special Administrative Region, China (RGC project No. HKU 7102/08E).

REFERENCES

Aalami BO (1998) Time-dependent analysis of concrete structures. *Progress in Structural Engineering and Materials* **1(4)**: 384–391.

Ariyawardena N and Ghali A (2002) Prestressing with unbonded internal or external tendon: analysis and computer model. *Journal of Structural Engineering* **128(12)**: 1493–1501.

Au FTK and Si XT (2011) Accurate time-dependent analysis of concrete bridges considering concrete creep, concrete shrinkage and cable relaxation. *Engineering Structures* **33(1)**: 118–126.

Au FTK, Liu CH and Lee PKK (2007) Shrinkage analysis of reinforced concrete floors using shrinkage-adjusted elasticity modulus. *Computers and Concrete* **4(6)**: 477–497.

Au FTK, Liu CH and Lee PKK (2009) Creep and shrinkage analysis of reinforced concrete frames by history-adjusted and shrinkage-adjusted elasticity moduli. *Structural Design of Tall and Special Buildings* **18(1)**: 13–35.

Bažant ZP (1972) Prediction of concrete creep effects using age-adjusted effective modulus method. *ACI Journal* **69(4)**: 212–217.

BSI (1997) BS 8110: Part 1: Structural use of concrete. BSI, London, UK.

BSI (2005) BS EN 1992: Part 2: Design of concrete structures. BSI, London, UK.

CEB (Comité Euro-International du Béton) (1993) *CEB-FIP Model Code 1990*. Thomas Telford, London, UK.

Elbadry MM and Ghali A (2001) Analysis of time-dependent effects in concrete structures using conventional linear computer programs. *Canadian Journal of Civil Engineering* **28(2)**: 190–200.

Ghali A and Neville AM (1989) *Structural Analysis: A Unified Classical and Matrix Approach*, 3rd edn. Chapman & Hall, New York, NY, USA.

Ghali A and Trevino J (1985) Relaxation of steel in prestressed concrete. *Journal of Prestressed Concrete Institute* **30(5)**: 82–94.

Ghali A, Favre R and Elbadry MM (2002) *Concrete Structures: Stresses and Deformations*, 3rd edn. Spon Press, London, UK.

Logan DL (2001) *A First Course in the Finite Element Method*, 4th edn. Thomson Learning, London, UK.

Magura DD, Sozen MS and Siess CP (1964) A study of stress relaxation in prestressing reinforcements. *Journal of Prestressed Concrete Institute* **9(2)**: 13–57.

Sharif A, Taher SF and Basu PK (1993) Time-dependent losses in prestressed continuous composite beams. *Journal of Structural Engineering* **119(11)**: 3151–3168.

Tadros MK, Ghali A and Dilger WH (1975) Time-dependent prestress loss and deflection in prestressed concrete members. *Journal of Prestressed Concrete Institute* **20(3)**: 86–98.

Youakim SA, Ghali A, Hida SE and Karbhari VM (2007) Prediction of long-term prestress losses. *Journal of Prestressed Concrete Institute* **52(2)**: 116–130.